

## Research Article

# Considering Variable Road Geometry in Adaptive Vehicle Speed Control

Xinping Yan,<sup>1</sup> Rui Zhang,<sup>1</sup> Jie Ma,<sup>1</sup> and Yulin Ma<sup>2</sup>

<sup>1</sup> Intelligent Transport Systems Research Center, Engineering Research Center for Transportation Safety (Ministry of Education), Wuhan University of Technology, Wuhan 430063, China

<sup>2</sup> Department of Automobile Engineering, Academy of Military Transportation, Tianjin 300161, China

Correspondence should be addressed to Rui Zhang; zhangrui318@163.com

Received 2 September 2013; Revised 4 November 2013; Accepted 4 November 2013

Academic Editor: Hui Zhang

Copyright © 2013 Xinping Yan et al. This is an open access article distributed under the Creative Commons Attribution License, which permits unrestricted use, distribution, and reproduction in any medium, provided the original work is properly cited.

Adaptive vehicle speed control is critical for developing Advanced Driver Assistance Systems (ADAS). Vehicle speed control considering variable road geometry has become a hotspot in ADAS research. In this paper, first, an exploration of intrinsic relationship between vehicle operation and road geometry is made. Secondly, a collaborative vehicle coupling model, a road geometry model, and an AVSC, which can respond to variable road geometry in advance, are developed. Then, based on  $H_{\infty}$  control method and the minimum energy principle, a performance index is specified by a cost function for the proposed AVSC, which can explicitly consider variable road geometry in its optimization process. The proposed AVSC is designed by the Hamilton-Jacobi Inequality (HJI). Finally, simulations are carried out by combining the vehicle model with the road geometry model, in an aim of minimizing the performance index of the AVSC. Analyses of the simulation results indicate that the proposed AVSC can automatically and effectively regulate speed according to variable road geometry. It is believed that the proposed AVSC can be used to improve the economy, comfort, and safety effects of current ADAS.

## 1. Introduction

At present, Advanced Driver Assistance Systems (ADAS) has become a hotspot in intelligent transportation systems (ITS) research area. There are many ADAS that have been or are being developed, including Adaptive Cruise Control System (ACC), which regulates the speed with the target vehicle spacing [1], Intelligent Speed Adaptive System (ISA), which regulates the speed with speed limit signs and marking, and Lane Keeping Assist Systems (LKAS) and Lane Departure Warning System (LDWS) that maintain a safe lane position, the vehicle orientation and among others [2]. Such systems either regulate vehicle operation or even directly control vehicle speed according to road geometry, such as traffic signs, pavement, and sight distance.

The literature review indicates that variable road geometry is mainly presented as changing road shapes. Accident rate of rear-end collision and rollover are still high, especially for those “dangerous locations,” such as long steep slopes, sharp

curves, and irregular road surface. Several reasons contribute to this. On one hand, speeding and the inherent limitations of vehicular sensor system in vision, sensitivity, and delay are widespread. On the other hand, variable road geometry is commonly not considered within ADAS. This results in that ADAS equipped vehicles cannot comprehensively “know” the road ahead and therefore they cannot develop an “optimal” vehicle operation in response to variable road geometry. Related studies show that considering variable road geometry can effectively improve the safety, comfort, and economy of vehicle operation.

Vehicle speed control is an important part of ADAS. Typically, the traditional methods of speed control are static in that they mostly specify one speed limit for a given road condition (e.g., sharp curve or steep slope), regardless of the relative location of the vehicle and road features (e.g., the beginning or the ending portion of a curve or a slope). In order to precisely control the vehicle speed on variable road geometry, most researches focus on road

geometrical features extraction and estimation. As the road features, such as slope, curvature, bank angle, are not easy to get by vehicular sensors available, road features estimation mainly adopts direct observers such as Kalman, Luenberger, or other observers based on proportional-integral, fuzzy, and sliding mode control [3]. Moreover, recent studies tend to collect road and environment information within a limited distance ahead. However, the methods proposed above over-rely on online data acquisition and processing and unknown data that need to be predictable but by a high cost of measurement, which results in that the real time of algorithm cannot be achieved easily [4]. For these reasons, limited researches tried to explore adaptive speed control method on variable road geometry. With the development of Cooperative Vehicle Infrastructure Systems (CVIS), real-time and abundant information about vehicle inside and outside, especially road geometry information, can be obtained by GPS, GIS, mobile communications, digital map, and so forth, which can support the development of adaptive vehicle speed controller (AVSC) in order to respond to variable road geometry [5]. AVSC can collect road information of entire road features (e.g., a curve or a slope) and make more informative and comprehensive decisions in the control of vehicle speed.

The literature review indicates that few researches have been focused on AVSC considering variable road geometry. Németh and Gáspár [6] introduced road division into vehicle modeling and added appropriate weighting factor for the reference velocity in each road section. They used LPV/ $H_\infty$  control method to design a velocity tracking controller on the slope road. The controller cannot only adjust the speed quickly and effectively on the slope but also reduce the frequent operations of the vehicle actuator. For the platooning vehicle on the slope, Németh and Gáspár [7] also adopt the above idea, which still adopts LPV/ $H_\infty$  control method to design a velocity tracking controller for the leader and string stable controller for each vehicle in the platoon. However, the slope angle in these references is still taken as the external disturbance, and the cruise/platooning system is guaranteed just by LPV method to keep the robustness for the change of the slope angle and uncertain factors.

Kamal et al. [8, 9] designed an ecological driving system for running a vehicle on roads with up-down slopes. This ecological system makes full use of the road information obtained from digital road maps and proposed a nonlinear model predictive control method to derive the vehicle control inputs by road terrain, vehicle dynamics, and fuel consumption characteristics. They acquired the complete road feature data including slope angle and the rate of slope angle, developed a fuel consumption model, and designed the optimal speed controller. This method mainly starts with driving economy on a slope road, but it does not consider vehicle running on a curve road as well as its safety and comfort on variable road geometry. In addition, other researches usually take road features as external disturbances and used the weight factors to eliminate the influence of disturbances, or simply ignore these road geometrical features [10, 11].

In China, Wang and Ma [12] developed the vehicle speed and spacing model on a curve and/or a slope road. But these

models are mainly suitable for macroscopic traffic flow simulation, and it is difficult to reflect the individual vehicle difference, that is, how vehicle regulates its own speed fitting in with variable road geometry. Zhang et al. [13] conducted a comprehensive research on ACC vehicles, such as driveline simplification, actuator design, acceleration switch, disturbance decoupling on the uncertainty parameters and nonlinear model, and fuel consumption analysis. Currently, they have done some researches on the ACC vehicle on a curve road to prevent vehicle from sideslip and rollover. Zhang combined ACC and Direct Yaw Control (DYC) together to put forward a curve coordinate controller, which not only can satisfy the longitudinal tracking for vehicles, but also can ensure the lateral stability of vehicles. However, in curve road, although the controller separates the ego and adjacent lanes effectively, it does not fundamentally consider the speed adaption on the curve road. In addition, there is rare report on AVSC on variable road geometry both at home and abroad.

Many control algorithms such as PID and LQ algorithms are required for online identification of controlled object, so precise mathematical model of object/process is essential by using these algorithms. However, the nonlinear, time varying and uncertain vehicle systems retrain the development of precise modeling of a vehicle. The approach used in this paper is the  $H_\infty$  optimization algorithm.

The study of  $H_\infty$  optimization algorithm has been of great interest, and many results can be found in the literature. To mention a few, the problem of filtering is investigated in [14–16], and the problem of model reduction is considered in [17]. The problem of the  $H_\infty$  step tracking control for discrete-time nonlinear systems is analyzed in [18–20]. The problem of robust static output feedback controls for networked control systems (NCSs) subject to network-induced delays and missing data are studied in [21]. Moreover, the  $H_\infty$  control has been also paid considerable attention and many results have been reported in automotive systems. For instance, lateral control of autonomy vehicle by using both  $H_\infty$  control and fuzzy control is studied in [22] to confirm that the control algorithm is feasible for practical application, and longitudinal control of electric vehicle by using  $H_\infty$  robust control is investigated in [23] to enhance the riding comfort and energy saving for vehicle constant speed cruise, especially in slope road. However, the road geometry features are used as disturbance or constant values to controller. To the best of the authors' knowledge, little cost function of  $H_\infty$  control has been developed by road geometry model. In this study, based on  $H_\infty$  Control Method and Hamilton-Jacobi Inequality (HJI) theory, a performance index is specified by a proposed cost function for the proposed AVSC, which can explicitly consider variable road geometry in its optimization process. The proposed AVSC is to make more informative and comprehensive decisions in the control of vehicle speed.

The rest of this paper develops as the following. After a literature review for adaptive speed control on variable road geometry is conducted, a collaborative vehicle coupling model and road geometrical model are presented in detail; an adaptive vehicle speed controller (AVSC) for variable road geometry consisting of upslope and a curve scenario

by using  $H_\infty$  and HJI method is described. And then simulation results are carried out and presented to illustrate the safety, comfort, and economy of the proposed AVSC. Finally, conclusions and further works are provided.

## 2. Methodology

Vehicle dynamic characteristics and road geometrical features are necessary in determining the risk behaviors of vehicle collision or rollover. Vehicle running on the slope needs to consider both vehicle dynamic parameters and road geometrical parameters, such as longitudinal acceleration, traction force, velocity, and slope angle. Vehicle running on the curve needs to consider lateral acceleration, yaw rate, steering wheel angle, and road curvature. Besides, a coupling relationship exists between longitudinal and lateral vehicle movements; a collaborative vehicle coupling model and road geometry model have been studied to accurately describe vehicle driving characteristics on the variable road geometry, thus improving the controller designed for AVSC.

**2.1. Vehicle Coupling Model.** The vehicle dynamics model with three degrees of freedom including longitudinal, lateral, and yaw motion can be developed by Newton's vector method. Besides, the operation conditions of vehicle usually need to fit in with different road geometries. So, the vehicle model should firstly consider the dynamic coupling between the lateral and longitudinal, followed by a full impact that road geometrical features have on the vehicle model. The model is referred to [24, 25] as shown below:

$$\begin{aligned}\dot{v}_x &= a_1 v_x^2 + v_y \dot{\psi} + C_f \frac{v_y + l_f \dot{\psi}}{m v_x} \delta - \mu g + \frac{F - C_f \delta}{m}, \\ \dot{v}_y &= -a_2 \frac{v_y}{v_x} - \left( v_x + \frac{k a_3}{v_x} \right) \dot{\psi} + \frac{F - \mu \lambda (mg - k_L v_x^2) + C_f \delta}{m} \delta, \\ \ddot{\psi} &= -a_4 \frac{\dot{\psi}}{v_x} - a_3 \frac{v_y}{v_x} + \frac{l_f}{I_z} \left( \frac{F - \mu \lambda (mg - k_L v_x^2) + C_f \delta}{m} \right),\end{aligned}\quad (1)$$

where

$$\begin{aligned}a_1 &= \frac{\mu k_L - k_D}{m}, \\ a_2 &= \frac{(C_f + C_r)}{m}, \\ a_3 &= \frac{(C_f l_f - C_r l_r)}{I_z},\end{aligned}$$

$$\begin{aligned}a_4 &= \frac{(C_f l_f^2 + C_r l_r^2)}{I_z}, \\ \lambda &= \frac{l_r}{l_f + l_r}, \\ k &= \frac{I_z}{m},\end{aligned}\quad (2)$$

and the vehicle parameters used are listed in Table 1.

In order to accurately define road geometrical features, such as slope, bank, and curvature, it is assumed that the orientation of the road surface is obtained from the horizontal position by a rotation around the vehicle's lateral axis equal to the slope angle  $\theta_s$  and a subsequent rotation around the longitudinal axis equal to the bank angle  $\theta_b$ . The slope angle and bank angle cause gravity components to appear in vehicle model, yielding

$$\begin{aligned}\dot{v}_x &= a_1 v_x^2 + v_y \dot{\psi} + C_f \frac{v_y + l_f \dot{\psi}}{m v_x} \delta + \frac{F - C_f \delta}{m} \\ &\quad - \mu g \cos \theta_s \mp g \sin \theta_s, \\ \dot{v}_y &= -a_2 \frac{v_y}{v_x} - \left( v_x + \frac{k a_3}{v_x} \right) \dot{\psi} + \frac{F - \mu \lambda (mg - k_L v_x^2) + C_f \delta}{m} \delta \\ &\quad - g \cos \theta_s \sin \theta_b.\end{aligned}\quad (3)$$

Then the road curvature is considered. As the road curvature and vehicle motion are not in the same coordinate system, the road curvature cannot be used directly by the vehicle model. Secondly, the bank angle is not easy to get, compared with road altitude and curvature got by digital map or other on board sensors. Last but not least, each lane of road has a certain width and an appropriate deviation is allowed in terms of the lateral motion of vehicle. So, a vehicle lateral deviation model is given here. In order to achieve a better ride comfort, the lateral deviation of the vehicle is defined as the lateral distance  $y_s$  from the mounting location of vehicle sensors to the road centerline, rather than the lateral distance  $y$  from the vehicle center of gravity (c.o.g) to the road centerline, as shown in Figure 1.

Assume that  $\psi_r$  is the angle between road centerline and the longitudinal axis of vehicle, and  $d_s$  is the horizontal distance between the road centerline and the vehicle longitudinal axis in radians. The approximate relationship between  $y_s$ ,  $y$  and  $\psi_r$  is

$$\sin \psi_r = \frac{y_s - y}{d_s} \approx \psi_r, \quad (4)$$

where  $d_s$  is the horizontal distance to the sensor from c.o.g.

Time differentiating (4), we get

$$\begin{aligned}\dot{y}_s &= \dot{y} + d_s \dot{\psi}_r, \\ \ddot{y}_s &= \ddot{y} + d_s \ddot{\psi}_r.\end{aligned}\quad (5)$$

TABLE 1: Vehicle parameters.

Parameters	Description
$m/\text{kg}$	Total mass
$I_z/\text{kg}\cdot\text{m}^2$	Yaw inertial
$l_f/\text{m}$	Distance from front axle to center of gravity
$l_r/\text{m}$	Distance from rear axle to center of gravity
$C_f/\text{N}\cdot\text{rad}^{-1}$	Front cornering stiffness
$C_r/\text{N}\cdot\text{rad}^{-1}$	Rear cornering stiffness
$\mu$	Rolling friction coefficient
$k_D/\text{N}\cdot\text{s}^2\cdot\text{m}^{-2}$	Aerodynamic drag parameter
$k_L/\text{N}\cdot\text{s}^2\cdot\text{m}^{-2}$	Aerodynamic lift parameter
$g/\text{m}\cdot\text{s}^{-2}$	Gravity acceleration
$F_{yf}F_{yr}/\text{N}$	Tire lateral force
$F_{xf}F_{xr}/\text{N}$	Tire longitudinal force
$\delta/\text{rad}$	Steering wheel angle

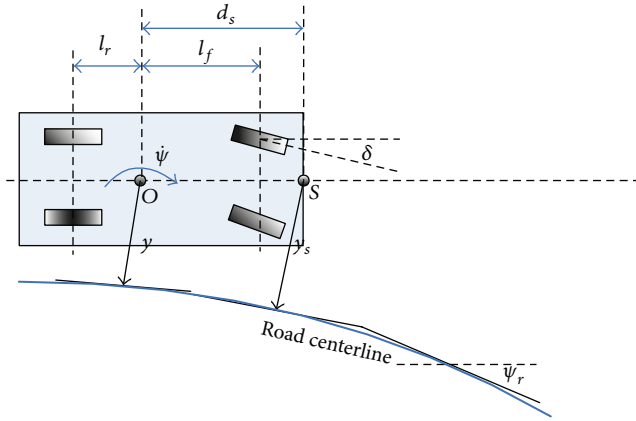


FIGURE 1: Vehicle lateral deviation model in terms of sensor space.

Let  $\psi_d$  be the yaw rotation of the road centerline with respect to the fixed earth frame, allowing us to write

$$\psi = \psi_r + \psi_d. \quad (6)$$

Time differentiating (6), we get

$$\begin{aligned} \dot{\psi}_r &= \dot{\psi} - \dot{\psi}_d, \\ \ddot{\psi}_r &= \ddot{\psi} - \ddot{\psi}_d, \end{aligned} \quad (7)$$

where  $\dot{\psi}_d = C v_x$ ; it should achieve an absolute desired yaw rate of  $C v_x$ , for a vehicle follows a curve with road curvature  $C$  (radius of curvature  $R = 1/C$ ).

Substituting  $\psi_r$  and its derivatives from (6) and (7) for (5), we get the vehicle lateral deviation model in the sensor space as

$$\begin{aligned} \dot{y}_s &= \dot{y} + d_s (\dot{\psi} - C v_x), \\ \ddot{y}_s &= \ddot{y} + d_s (\ddot{\psi} - \ddot{\psi}_d). \end{aligned} \quad (8)$$

Consistent with the road conditions, it can be reasonably assumed that the roadway can be described by a series of curves that have a constant road curvature. Because the road curvature is piecewise continuous, it can be assumed that  $\ddot{\psi}_d \approx 0$  [26].

In summary, according to the vehicle coupling model with regard to road geometrical features, on one hand, the vehicle still needs to overcome the action of gravity caused by the slope angle in the longitudinal control. On the other hand, the vehicle also needs to mitigate the change of deviation caused by the road curvature in the lateral control. In addition, it is necessary to analyze the speed performance caused by the changes of variable road geometries.

**2.2. Road Geometry Model.** According to road design rules, road geometry determines the direction and specific location of the route. Road geometry can reach the best combination by integrated design of the road shapes including horizon, vertical, and cross sections, which can meet not only driver visual and psychological requirements, but also vehicle dynamics and kinematics characteristics, thus reducing the driving work and improving the driving safety, comfort, and economy. Clothoid curves have been used for road geometry design in order to geometrically join a straight road to a curve road, or a straight road to a slope road [3, 27, 28]. Besides, vertical curves should be used to geometrically join an uphill and a downhill road. As the example of curve road, the main characteristic of a clothoid function is that its curvature is proportional to the length of the curve measured from its origin

$$C(l) = C_0 + C_1 \cdot l, \quad (9)$$

where  $C_0$  and  $C_1 = dC/dl$  are the curvature and rate of curvature of the road, respectively;  $l$  is the curve length.

Then, the heading direction  $\varphi(l)$  is got by the first integral of the curvature

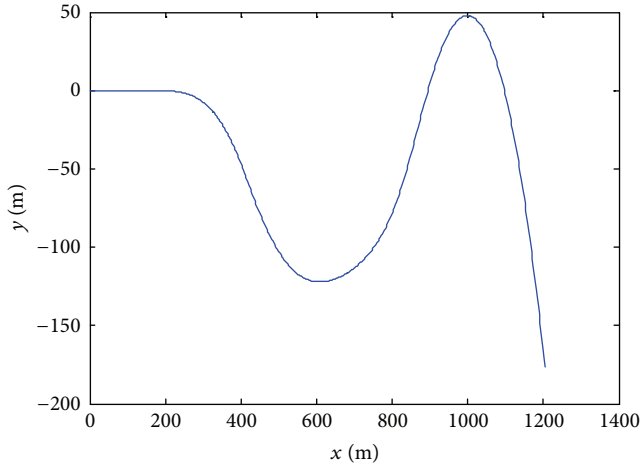
$$\varphi(l) = \varphi_0 + \int_0^l C(\tau) d\tau = \varphi_0 + C_0 l + \frac{1}{2} C_1 l^2. \quad (10)$$

And the second integral represents the curve's longitudinal distance  $x(l)$  and lateral distance  $y(l)$

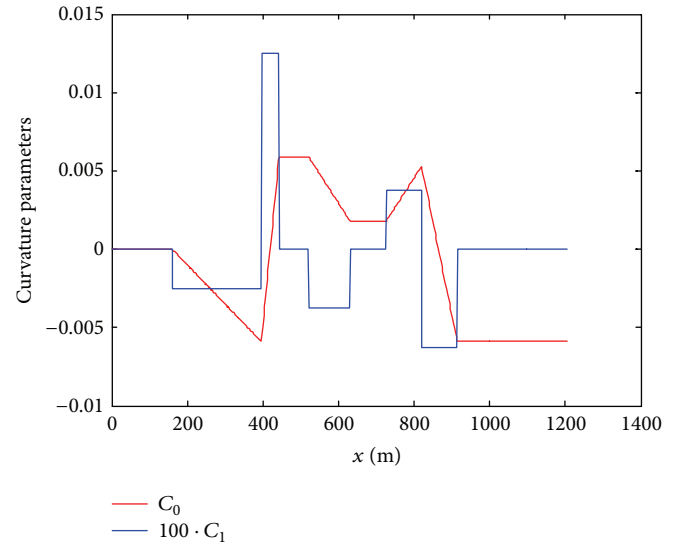
$$\begin{aligned} x(l) &= x_0 + \int_0^l \cos \varphi(\tau) d\tau, \\ y(l) &= y_0 + \int_0^l \sin \varphi(\tau) d\tau. \end{aligned} \quad (11)$$

Assuming  $\sin \varphi \approx \varphi$ ,  $\cos \varphi \approx 1$ , (11) is rewritten as

$$\begin{aligned} x(l) &= x_0(l) + l, \\ y(l) &= y_0 + \varphi l + \frac{1}{2} C_0 l^2 + \frac{1}{6} C_1 l^3. \end{aligned} \quad (12)$$

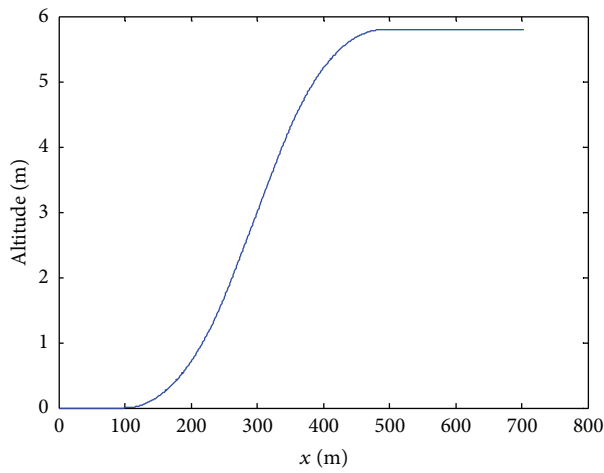


(a) Simulated curve road

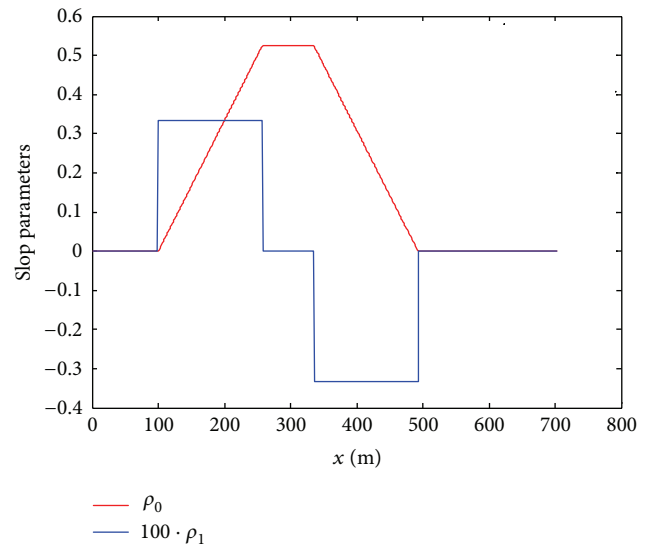


(b) Curvature parameters

FIGURE 2: Simulated curve road with curvature parameters.



(a) Simulated slope road



(b) Slope parameters

FIGURE 3: Simulated slope road with slope parameters.

If  $x_0(l) = 0$  leads to  $x(l) = l$ , the curve's lateral distance  $y(x)$  and the head direction  $\varphi(x)$  can be given as

$$\begin{aligned}\varphi(x) &= \varphi_0 + C_0 x + \frac{1}{2} C_1 x^2, \\ y(x) &= y_0 + \varphi x + \frac{1}{2} C_0 x^2 + \frac{1}{6} C_1 x^3.\end{aligned}\quad (13)$$

Figure 2 gives a simulated curve road with curvature parameters  $C_0$  and  $C_1$  by this curve road model.

Similarly, in slope modeling, we can substitute the slope angle  $\rho_0$  and its rate  $\rho_1$  for  $C_0$  and  $C_1$ , respectively, and also substitute the horizontal and vertical distance for the

longitudinal and lateral distances, respectively, so the vertical distance  $z(x)$  and the head direction  $\varphi(x)$  also can be given as

$$\begin{aligned}\varphi(x) &= \varphi_0 + \rho_0 x + \frac{1}{2} \rho_1 x^2, \\ z(x) &= z_0 + \varphi x + \frac{1}{2} \rho_0 x^2 + \frac{1}{6} \rho_1 x^3.\end{aligned}\quad (14)$$

Figure 3 gives a simulated slope road with slope parameters  $\rho_0$  and  $\rho_1$  by this curve road model.

Seen from road geometry model developed above, these road geometrical features, such as  $C_0$  and  $C_1$ , or  $\rho_0$  and



$\rho_1$ , can represent the direction and location of a curve or a slope, and the derivation has shown a great deal of similitude between these road features and vehicle parameters, such as acceleration, velocity, and displacement. Hence, if the control system of vehicle makes full use of these road features and vehicle parameters, AVSC can be achieved.

### 3. AVSC Design

According to the collaborative vehicle coupling model and road geometry model, we combine (1), (3), and (8), yielding

$$\begin{aligned} \dot{v}_x &= a_1 v_x^2 + v_y \dot{\psi} + C_f \frac{v_y + l_f \dot{\psi}}{m v_x} \delta + \frac{F - C_f \delta}{m} \\ &\quad - \mu g \cos \theta_s \mp g \sin \theta_s, \\ \ddot{y}_s &= - (a_2 + d_s a_3) \frac{\dot{y}_s}{v_x} - \left( v_x + \frac{k a_3 - d_s (a_2 - a_4) - d_s^2 a_3}{v_x} \right) \dot{\psi} \\ &\quad + \left( 1 + \frac{d_s l_f}{I_z} \right) \frac{F - \mu \lambda (m g - k_L v_x^2) + C_f}{m} \delta \\ &\quad - C (d_s a_2 + d_s^2 a_3). \end{aligned} \quad (15)$$

As the lateral deviation model needs lateral and yaw motion information, and both lateral and yaw motion share the same control input, the only two independent states have been controlled.

Assuming that brake, throttle, and steering dynamics are discounted, we make some transformation for inputs of state equation of the vehicle system

$$\begin{aligned} u_1 &= C_f \frac{v_y + l_f \dot{\psi}}{m v_x} \delta + \frac{F - C_f \delta}{m}, \\ u_2 &= \frac{F - \mu \lambda (m g - k_L v_x^2) + C_f}{m} \delta. \end{aligned} \quad (16)$$

Thus, we have only to design proper AVSC law to compute the inputs of the vehicle system  $F$  ( $\delta$ , resp.) as the traction/braking force (the steering wheel angle, resp.).

Then, the collaborative vehicle coupling model and road geometry model can be got as a form of state

$$\begin{aligned} \dot{x}_1 &= a_1 x_1^2 + x_2 x_3 + u_1 - \mu g \cos \theta_s - g \sin \theta_s = f(x, u_1, \theta_s), \\ \dot{x}_2 &= - (a_2 + a_3 d_s) \frac{x_2}{x_1} \\ &\quad - \left( x_1 + \frac{k a_3 - d_s (a_2 - a_4) - d_s^2 a_3}{x_1} \right) x_3 \\ &\quad + \left( 1 + \frac{d_s l_f}{I_z} \right) u_2 - C (d_s a_2 + d_s^2 a_3) = f(x, u_2, C). \end{aligned} \quad (17)$$

Among them  $\mathbf{x}[x_1, x_2, x_3]$  is the state variables of vehicle control system, and  $[x_1, x_2, x_3] = [v_x, v_y, \dot{\psi}]$ ,  $\theta_s$  is the road slope angle, and  $C$  is the road curvature.

$H_\infty$  control theory is to analyze the stability of a system in terms of energy dissipation. If a system is activated, its stored energy will be attenuated gradually with time. When it reaches the equilibrium state, its energy is at the minimum value, and we can say that the system is asymptotically stable.  $H_\infty$  method presents an objective function about tracking error or control cost and designs a suitable feedback controller so that the closed loop system is stable with the  $H_\infty$  norm of its transfer function minimum or less than a constant. Among them, the criterion of  $H_\infty$  method can be seen as a nonlinear optimal control problem considering the performance index below:

$$\min_u \int_0^\infty (\|u(t)\|^2 + L(x)) dt, \quad (18)$$

where  $L$  is the cost function,  $L(x) \geq 0$ , and  $L(0) = 0$ .

In this formulation, the cost function  $L$  is considered to have the following form:

$$L = \lambda_1 \Phi_1 + \frac{\lambda_2}{2} \Phi_2^2 + \lambda_3 \left[ \frac{1}{2} (x_1 - v_d)^2 \right], \quad (19)$$

where

$$\begin{aligned} \Phi_1 &= \begin{cases} \frac{\varphi x + (1/2) \rho_0 x^2 + (1/6) \rho_1 x^3}{x_1} & \text{slope} \\ \frac{\varphi x + (1/2) C_0 x^2 + (1/6) C_1 x^3}{x_1} & \text{curve} \end{cases} \\ \Phi_2 &= \begin{cases} a_x + g \sin \theta_s & \text{slope} \\ a_y + d_s (\ddot{\psi} - C \dot{x}_1) & \text{curve.} \end{cases} \end{aligned} \quad (20)$$

The cost function consists of three terms, each of which is multiplied by a constant weight  $\lambda_1$ ,  $\lambda_2$ , and  $\lambda_3$ , respectively. The first term defines the cost in terms of speed changes caused by road geometrical features. In a curve road, it can be computed from (13) as  $y(x)/x_1$  and setting  $y_0 = 0$ . In a slope road, it can be computed from (14) as  $z(x)/x_1$  and setting  $z_0 = 0$ . The second term is the cost that corresponds to the longitudinal and lateral acceleration forces on the vehicle, respectively, considering the counteracting effect of gravitational force on the vehicle due to the road slope from (3) and that of yaw moment on the vehicle due to the road curvature from (8), respectively. The last term is the cost for not running at the given speed on the road  $v_d$ . The weights are chosen in such a way that the usual magnitudes of the cost terms are balanced with respect to others. Finally, the weights can be fine-tuned through observation of simulation results to maximize the performance of controller.

In order to derive the optimal control inputs, the Hamiltonian function is formed using (17)–(19) as follows:

$$H_i(x, p_i, \varphi_i, u_i) = p_i^T f(x, u_i, \varphi_i) + L_i(x, u_i), \quad (21)$$

where  $i$  is the different road geometry, such as slope or curve,  $p$  is costate, and  $\varphi$  is road geometrical features, such as slope angle  $\theta_s$  or curvature  $C$ .

Let  $f(x, u, \varphi) = f(x) + g(x)u + k(x)\varphi$ , according to the Hamilton-Jacobi Inequality (HJI), if there is a non-negative function solution of  $V(x)$  of  $C^r$  class ( $r > 1$ ) satisfying

$$V_x(x) f(x) + \frac{1}{2} V_x(x) g(x) g^T(x) V_x^T(x) + \frac{1}{2} L(x) = 0. \quad (22)$$

Then the state feedback control law of  $C^{r-1}$  class can be obtained:

$$u = -g^T(x) V_x^T(x). \quad (23)$$

For this specific problem of deriving optimal control inputs, it is required to compute the following.

On a slope road

$$\begin{aligned} \frac{\partial H}{\partial \varphi} &= \frac{\partial}{\partial \varphi} H_i(x, p_i, \varphi_i, u_i) \\ &= \frac{\partial}{\partial \varphi} (p_i^T f(x, u_i, \varphi_i) + L_i(x, u_i)) \\ &= -p_2 g \cos \theta_s \dot{\theta}_s, \\ \theta_s(l) &= \tan^{-1} \left( \frac{R_{\text{alt}}(l + \Delta l) - R_{\text{alt}}(l - \Delta l)}{2\Delta l} \right), \\ \frac{d}{dl} \theta_s(l) &= \left( \frac{\theta_s(l + \Delta l) - \theta_s(l - \Delta l)}{2\Delta l} \right), \end{aligned} \quad (24)$$

$$(25)$$

where  $R_{\text{alt}}$  is altitude of road and  $l$  is mileage, and these data can be obtained by digital map.

On a curve road

$$\begin{aligned} \frac{\partial H}{\partial \varphi} &= \frac{\partial}{\partial \varphi} H_i(x, p_i, \varphi_i, u_i) \\ &= \frac{\partial}{\partial \varphi} (p_i^T f(x, u_i, \varphi_i) + L_i(x, u_i)) \\ &= -p_2 d_s \dot{x}_1 C C_1, \\ C &= \frac{1}{R}, \\ \dot{C} &= C_1, \end{aligned} \quad (26)$$

$$(27)$$

where  $R$  is curve radius and  $C_1$  is a constant, and these also can be obtained by digital map or actual measurement.

Last but not least, the constraint of driving comfort also needs to be considered (changes of longitudinal acceleration

TABLE 2: Vehicle parameters.

Parameters	Value
$m/\text{kg}$	2000
$I_z/\text{kg}\cdot\text{m}^2$	3150
$l_f/\text{m}$	1.33
$l_r/\text{m}$	1.26
$C_f/\text{N}\cdot\text{rad}^{-1}$	80000
$C_r/\text{N}\cdot\text{rad}^{-1}$	80000
$\mu$	0.02
$k_D/\text{N}\cdot\text{s}^2\cdot\text{m}^{-2}$	0.4
$k_L/\text{N}\cdot\text{s}^2\cdot\text{m}^{-2}$	0.005
$g/\text{m}\cdot\text{s}^{-2}$	9.8
$d_s/\text{m}$	2
$\lambda_1$	230
$\lambda_2$	220
$\lambda_3$	8

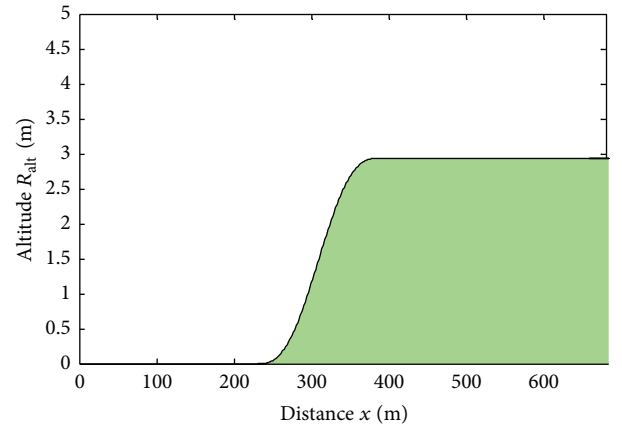


FIGURE 4: The simulation of the slope road.

and lateral acceleration within  $\pm 2 \text{ m/s}^2$ ,  $\pm 0.05 \text{ g m/s}^2$ ) in controller design. So, we can get

$$\dot{x}_{1,2} = \begin{cases} a_{\min} & (|\dot{x}_{1,2}| \leq |a_{\min}|), \\ a_{\max} & (|\dot{x}_{1,2}| \geq |a_{\max}|). \end{cases} \quad (28)$$

#### 4. AVSC Simulation

For the purpose of testifying the performance of designed AVSC, a series of simulation experiments combining the vehicle coupling model with the road geometry model are performed. The specific vehicle parameters are as shown in Table 2.

In simulation 1, a slope road is given first. The slope is shown in Figure 4, and its slope angle is calculated by (14) and (25), as shown in Figure 5.

Then, the AVSC simulation is made for this slope scenario. Assuming the initial speed  $v_d$  is  $79.2 \text{ km/h}$  ( $22 \text{ m/s}$ ), simulation lasts  $30 \text{ s}$ , and its sampling time is  $0.05 \text{ s}$ . First, the following two types of vehicle speed control, Adaptive Speed Control Driving (ASCD) and Constant Speed Driving

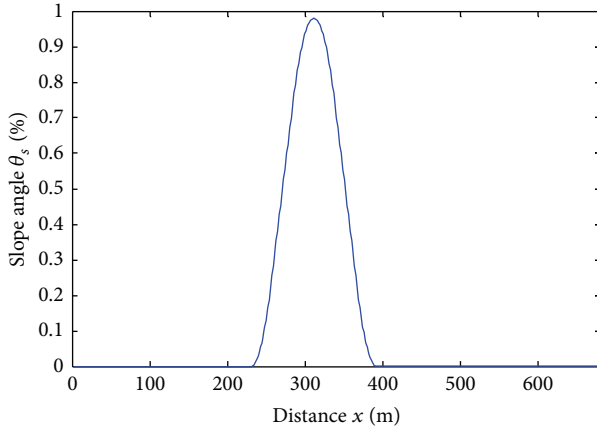


FIGURE 5: The calculation of the slope angle.

(CSD), are applied for a comparison analysis. CSD uses the information of the slope road to generate the control input so that the velocity remains constant, regardless of the changing of the slope. ASCD uses the proposed method in this paper to automatically regulate speed fitting in with the change of the slope road and, in this case, slope angle.

It can be seen from Figure 6(a) that with the vehicle entering slope with its initial speed, based on the defined cost function, the ASCD vehicle can reach the top of slope through an adaptive way with an operation profile of “pre-accelerating-post-decelerating.” Despite that the speed of the ASCD vehicle should not have little ups and downs in the early stages of running on the slope, maybe something wrong in computation of the cost function, it has a good, smooth running performance on the whole slope. But the CSD vehicle keeps the speed unchanged at the cost of a very high control input, easily making the actuators in danger.

Figure 6(b) shows the traction/braking forces under two types of speed control for the slope scenario. The forces of the CSD vehicle change greatly when it runs on the slope, while the forces of the ASCD vehicle move gently over the slope, depending on the location of the vehicle. That is because the cost functions of the ASCD take the slope angle and its changing rate into account, that is,  $\rho_0$  and  $\rho_1$ . Except for the final steady state, also seen in Figure 4(b), the forces of the ASCD remain stable for a period of time, due to the constraint of driving comfort from (28).

In addition, the performance of the two types of speed controllers is compared from the perspective of the control forces, which is calculated as the sum of absolute value of the entire traction/braking forces under the slope scenario ( $\sum|F|$ ). As shown in Figure 6(c), the total force of the CSD vehicle is 692,280 N, while that for the ASCD vehicle is 374,800 N. Therefore, it can be concluded that under the same slope and initial speed condition, the AVSC applied in this paper can reduce the consumption of the control energy by 45.86%.

In simulation 2, the curve road is given. Road radius can be obtained from (29), and the curvature can be obtained from (13) and (25), as shown in Figure 7.

Then, the AVSC simulation is made for this curve scenario. Assuming the initial speed is 90 km/h (25 m/s), the simulation also lasts 30 s, and its sampling time is 0.05 s. Both ASCD and CSD vehicles are still applied via the curve road for a comparison analysis. Therefore,

$$R = \begin{cases} 0, & 0 \leq x < 120, \\ 200, & 120 \leq x < 120 + 25\pi, \\ 400, & 120 + 25\pi \leq x < 120 + 100\pi, \\ 200, & 120 + 100\pi \leq x < 120 + 125\pi, \\ 0, & x \geq 120 + 125\pi. \end{cases} \quad (29)$$

In Figure 8(a), the ASCD vehicle runs via a curve in the same way as it runs on a slope. Based on the defined cost function, the ASCD vehicle can decrease when approaching the curve and accelerate when it is going to leave the curve. However, although the CSD vehicle keeps a constant speed through the curve, it is easy to result in a risky behavior of collision or rollover. Figure 8(b) shows the steering angle under two types of speed control. The steering angle of the CSD vehicle changes greatly when it runs through the curve, as the very reason for rollover. While the steering angle of the ASCD vehicle is very small, only one tenth of that of the CSD vehicle. In addition, the lateral velocity and the yaw rate are also fitting in with the road curvature as shown in Figures 8(c) and 8(d), respectively. For Figure 8(e), the initial horizontal position in this simulation is 0.2 m, in terms of sensor space  $y_s$ , rather than  $y$ , and the ASCD vehicle can maintain the lateral deviation minimum when leaving the curve, while the CSD vehicle need not only turn sharply, but also have the deviation kept within  $\pm 0.2$  m; thus it is difficult to meet the desired state.

In a summary, the ASCD vehicle can regulate the speed fitting in with the road geometrical features under AVSC design. Compared with the CSD vehicle, the ASCD vehicle has a proper, satisfactory performance of the longitudinal, lateral, and yaw control.

## 5. Conclusions and Future Works

A novel adaptive vehicle speed controller (AVSC) is presented in this paper. The AVSC proposed is developed based on a cost function and  $H_\infty$  control method and it is tested with a collaborative road geometrical model and vehicle coupling model. Both the developed collaborative model and the cost function of the AVSC consider variable road geometry and therefore are more accurate for simulating vehicle's performance. The proposed AVSC can regulate speed automatically fitting in with the changing road geometry; and has the advantages of improved safety, comfort, and economy.

Because the vehicle coupling model does not consider traction force and wheel angle, the simulations carried out in this paper only contain three state parameters as longitudinal velocity, lateral velocity, and yaw rate. In the future, the lateral deviation submodel used is mainly for lane changing and lane keeping purposes. A more realistic representation of acceleration, braking, and steering wheel operation still needs to be further studied in order to include traction/braking



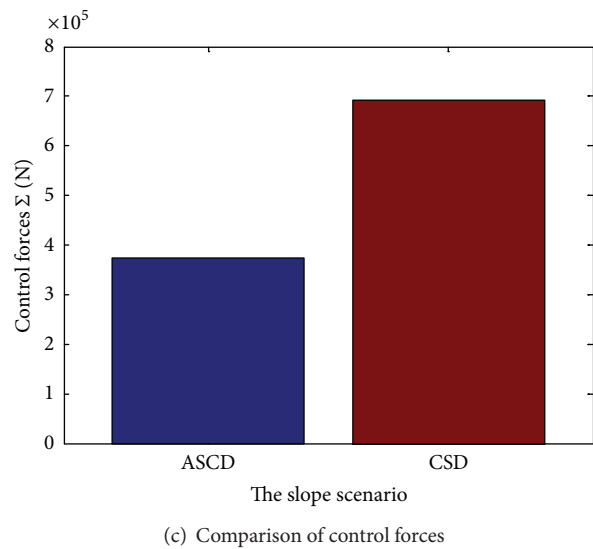
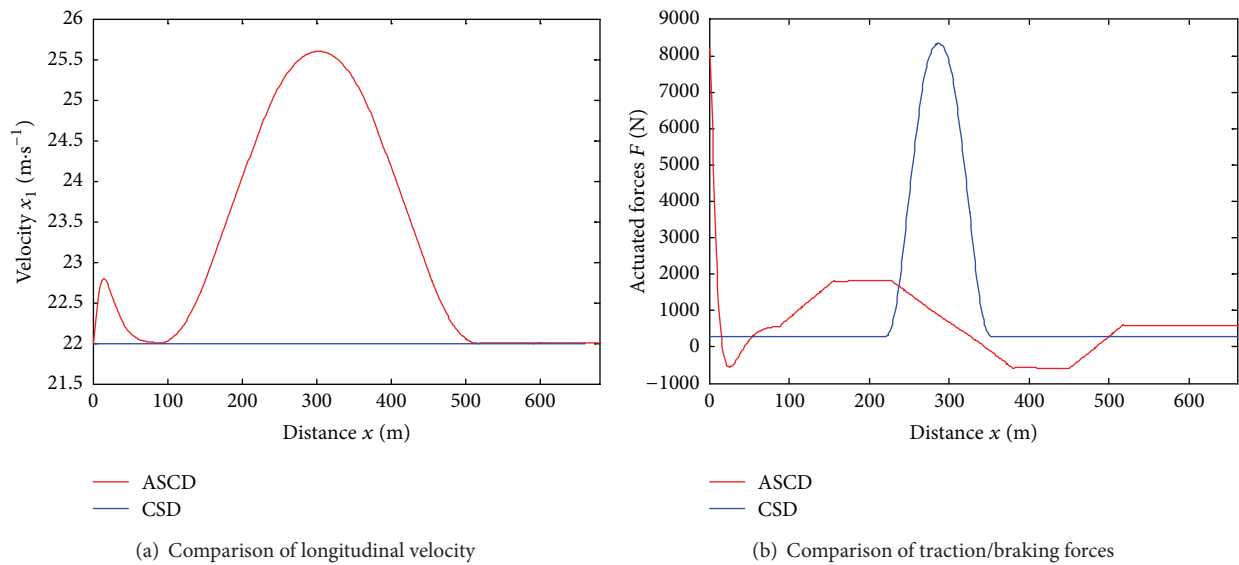


FIGURE 6: AVSC simulation on a slope road.

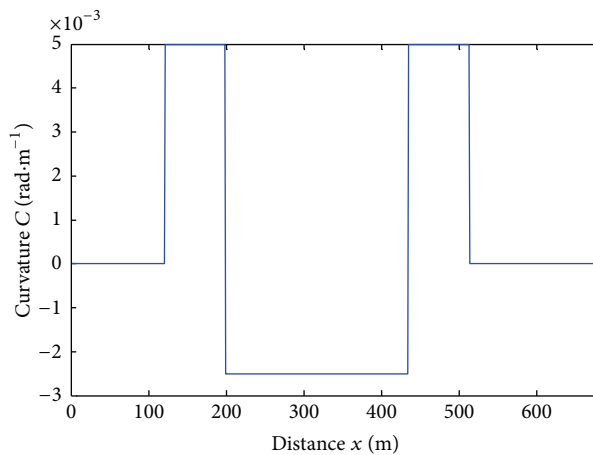
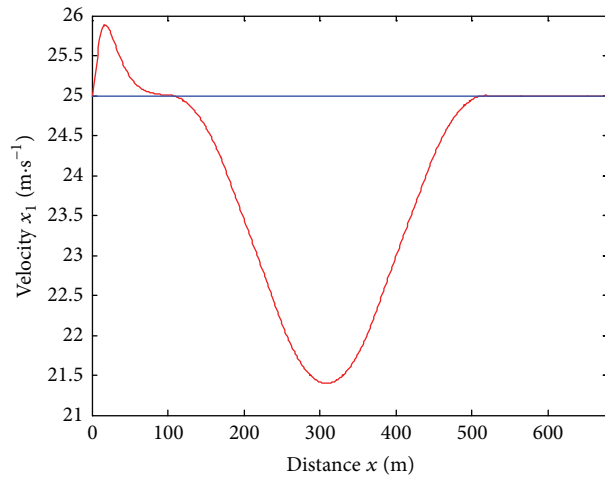
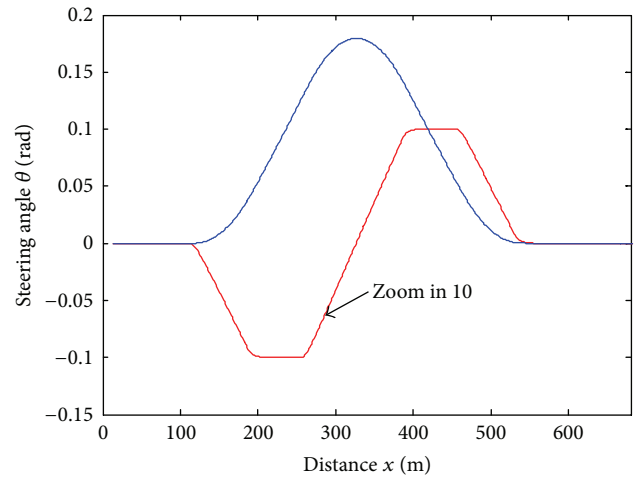


FIGURE 7: Road curvature.



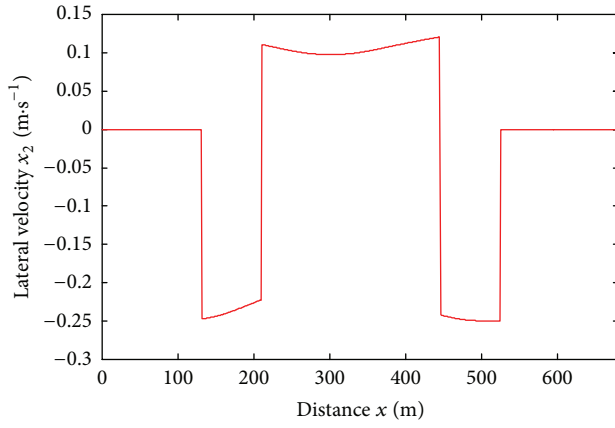
— ASCD  
— CSD

(a) Comparison of longitudinal velocity

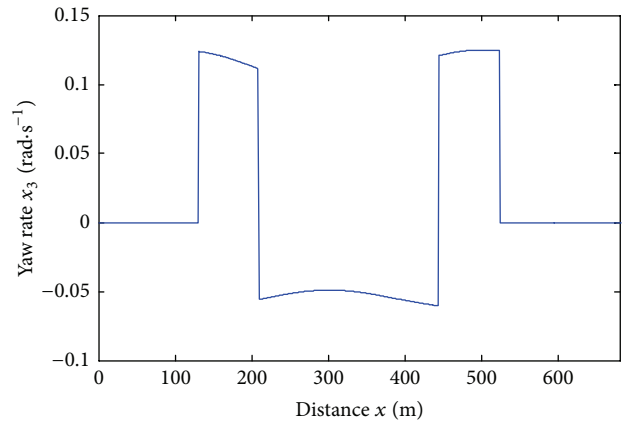


— ASCD  
— CSD

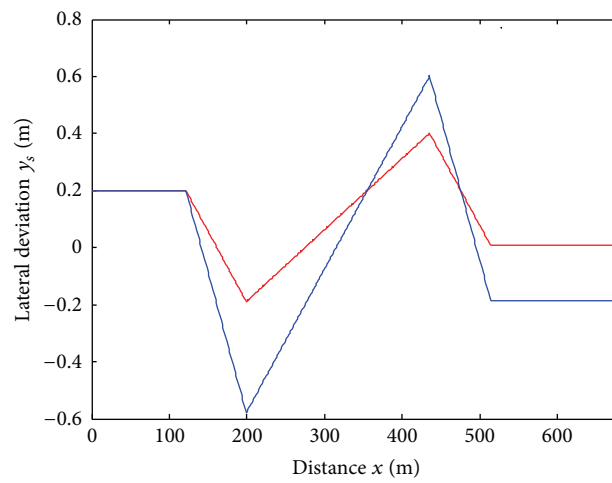
(b) Comparison of steering angle



(c) Lateral velocity profile



(d) Yaw rate profile



— ASCD  
— CSD

(e) Comparison of lateral deviation

FIGURE 8: AVSC simulations via a curve road.

force and front wheel angle into the lateral deviation sub-model.

## Conflict of Interests

The authors declare that there is no actual or potential conflict of interests regarding the publication of this paper.

## Acknowledgments

This study is supported by the National High-Tech R&D Program of China (863 Program) (no. 2011AA110402) and the National Natural Science Foundations of China (nos. 61203236 and 61174173).

## References

- [1] L. Xiao and F. Gao, "A comprehensive review of the development of adaptive cruise control systems," *Vehicle System Dynamics*, vol. 48, no. 10, pp. 1167–1192, 2010.
- [2] J. Piao and M. McDonald, "Advanced driver assistance systems from autonomous to cooperative approach," *Transport Reviews*, vol. 28, no. 5, pp. 659–684, 2008.
- [3] C. Lundquist and T. B. Schön, "Road geometry estimation and vehicle tracking using a single track model," in *Proceedings of the IEEE Intelligent Vehicles Symposium*, pp. 144–149, Eindhoven, The Netherlands, June 2008.
- [4] L. Guo, X. H. Huang, B. Y. Liu, and B. Li, "Curved road detection based on roadway design model," *Journal of Transport Information and Safety*, vol. 3, no. 30, pp. 141–146, 2012.
- [5] G. Toulminet, J. Boussuge, and C. Laurgeau, "Comparative synthesis of the 3 main European projects dealing with Cooperative Systems (CVIS, SAFESPOT and COOPERS) and description of COOPERS demonstration Site 4," in *Proceedings of the 11th International IEEE Conference on Intelligent Transportation Systems (ITSC '08)*, pp. 809–814, Beijing, China, December 2008.
- [6] B. Németh and P. Gáspár, "Design of vehicle platoon control based on predicted road inclinations," in *Proceedings of the IEEE/ASME International Conference on Advanced Intelligent Mechatronics (AIM '11)*, pp. 265–270, Budapest, Hungary, July 2011.
- [7] B. Németh and P. Gáspár, "Considering predicted road conditions in platoon control design," *Transportation Engineering*, vol. 39, no. 2, pp. 69–75, 2011.
- [8] M. A. S. Kamal, M. Mukai, J. Murata, and T. Kawabe, "Ecological vehicle control on roads with up-down slopes," *IEEE Transactions on Intelligent Transportation Systems*, vol. 12, no. 3, pp. 783–794, 2011.
- [9] M. A. S. Kamal, M. Mukai, J. Murata, and T. Kawabe, "Ecological driver assistance system using model-based anticipation of vehicle-road-traffic information," *IET Intelligent Transport Systems*, vol. 4, no. 4, pp. 244–251, 2010.
- [10] J. E. Naranjo, C. Gonzalez, R. Garcia, and T. Pedro, "Cooperative throttle and brake fuzzy control for ACC stop & go maneuvers," *IEEE Transactions on Vehicular Technology*, vol. 56, no. 4, pp. 1623–1630, 2007.
- [11] V. L. Bageshwar, W. L. Garrard, and R. Rajamani, "Model predictive control of transitional maneuvers for adaptive cruise control vehicles," *IEEE Transactions on Vehicular Technology*, vol. 53, no. 5, pp. 1573–1585, 2004.
- [12] H. Wang and S. F. Ma, "Car-following model and simulation with curves and slopes," *China Civil Engineering Journal*, vol. 38, no. 11, pp. 106–111, 2005.
- [13] D. Z. Zhang, K. Q. Li, and J. Q. Wang, "A curving ACC system with coordination control of longitudinal car-following and lateral stability," *Vehicle System Dynamics*, vol. 50, no. 7, pp. 1085–1102, 2012.
- [14] X. J. Su, P. Shi, L. G. Wu, and Y. D. Song, "A novel approach to filter design for T-S fuzzy discrete-time systems with time-varying delay," *IEEE Transactions on Fuzzy Systems*, vol. 20, no. 6, pp. 1114–1129, 2012.
- [15] W. B. Li, Y. Xu, and H. Z. Li, "Robust  $I_2$ - $I_\infty$  filtering for discrete-time Markovian jump linear systems with multiple sensor faults, uncertain transition probabilities and time-varying delays," *IET Signal Processing*, vol. 7, no. 8, pp. 710–719, 2013.
- [16] H. Zhang, Y. Shi, and A. S. Mehr, "Robust weighted  $H_\infty$  filtering for networked systems with multiple sensor faults," in *Proceedings of the 8th World Congress on Intelligent Control and Automation (WCICA '10)*, pp. 1228–1233, Jinan, China, July 2010.
- [17] X. J. Su, L. G. Wu, P. Shi, and Y. D. Song, " $H_\infty$  model reduction of takagi-sugeno fuzzy stochastic systems," *IEEE Transactions on Systems, Man, and Cybernetics B*, vol. 42, no. 6, pp. 1574–1585, 2012.
- [18] H. Zhang, Y. Shi, and M. X. Liu, "Step tracking control for networked discrete-time nonlinear systems with integral and predictive actions," *IEEE Transactions on Industrial Informatics*, vol. 9, no. 1, pp. 337–345, 2013.
- [19] H. Zhang, Y. Shi, M. Q. Xu, and H. T. Cui, "Observer-based tracking controller design for networked predictive control systems with uncertain markov delays," in *Proceedings of the American Control Conference*, pp. 5682–5687, Montréal, Canada, June 2012.
- [20] H. Zhang, Y. Shi, and B. X. Mu, "Optimal  $H_\infty$ -based linear-quadratic regulator tracking control for discrete-time takagi-sugeno fuzzy systems with preview actions," *Journal of Dynamic Systems, Measurement, and Control*, vol. 135, pp. 044501-1–044501-5, 2013.
- [21] H. Zhang, Y. Shi, and A. Saadat Mehr, "Robust static output feedback control and remote PID design for networked motor systems," *IEEE Transactions on Industrial Electronics*, vol. 58, no. 12, pp. 5396–5405, 2011.
- [22] L. Chen, J. Wang, and N. Li, " $H_\infty$  adaptive variable universe fuzzy control for autonomous vehicles," in *Proceedings of the 26th Chinese Control Conference (CCC '07)*, pp. 82–86, Zhangjiajie, China, July 2007.
- [23] Y. Hou and Z. Liu, "An  $H_2/H_\infty$  robust control approach to electric vehicle constant speed cruise," in *Proceedings of the 30th Chinese Control Conference (CCC '11)*, pp. 2384–2389, Yantai, China, July 2011.
- [24] R. Zhang, X. P. Yan, J. Ma, C. Z. Wu, and Y. L. Ma, "Design of intelligent vehicle speed adaption based on variable road geometry," in *Proceedings of the 2nd International Conference on Transportation Information and Safety*, pp. 1708–1714, Wuhan, China, June 2013.
- [25] Y. L. Ma, Q. Wu, X. P. Yan, and R. Zhang, "The hardware-in-the-loop simulator: a mechatronic testbed for cooperative vehicles maneuvers," *International Journal of Intelligent Transportation Systems Research*, vol. 11, no. 1, pp. 11–22, 2013.

- [26] S. Kumarawadu and T. T. Lee, "Neuroadaptive combined lateral and longitudinal control of highway vehicles using RBF networks," *IEEE Transactions on Intelligent Transportation Systems*, vol. 7, no. 4, pp. 500–512, 2006.
- [27] H. Dahmani, M. Chadli, A. Rabhi, and A. El Hajjaji, "Vehicle dynamics and road geometry estimation using a Takagi-Sugeno fuzzy observer with unknown inputs," in *Proceedings of the IEEE Intelligent Vehicles Symposium (IV '11)*, pp. 272–277, Baden-Baden, Germany, June 2011.
- [28] A. Hernandez-Gutierrez, J. I. Nieto, T. Bailey, and E. M. Nebot, "Probabilistic road geometry estimation using a millimetre-wave radar," in *Proceedings of the IEEE/RSJ International Conference on Intelligent Robots and Systems*, pp. 4601–4607, San Francisco, Calif, USA, September 2011.

